Journal of Statistical Physics, Vol. 107, Nos. 1/2, April 2002 (© 2002)

Lattice Boltzmann Solid Particles in a Lattice Boltzmann Fluid

Bastien Chopard[1, 2] **and Stefan Marconi**[1]

Received February 15, 2001; accepted November 16, 2001

We define a lattice Boltzmann model of solid, deformable suspensions immersed in a fluid itself described in terms of the lattice Boltzmann method. We discuss the rules governing the internal dynamics of the solid object as well as the rules specifying the interaction between solid and fluid particle. We perform a numerical drag experiment to validate the model. Finally we consider the case of a population of flexible chains in suspension in a shear stress flow and study the influence on the velocity profile.

KEY WORDS: Lattice; Boltzmann; fluid; deformable solid; mechanics; suspension.

1. INTRODUCTION

The lattice Boltzmann (LB) technique[1–3] is now widely used to simulate complex fluid flows.[4, 5] In this approach, the fluid is discretized on a lattice and is represented by distributions functions $N_k(\vec{r}, t)$ giving the density of fictitious fluid particles with velocity $\vec{v}_k$ entering lattice site $\vec{r}$ at discrete time t. The admissible velocities $\vec{v}_k$ are dependent of the lattice topology. Usually, k runs between 0 and z, where z is the lattice coordination number (i.e., the number of lattice links). By convention $\vec{v}_0 = 0$ and N_0 represents the density distribution of rest particles.

In the so-called non-thermal BGK model,[1, 3, 6, 2] the evolution of the density distribution is

$$N_k(\vec{r}+\tau\vec{v}_k, t+\tau) = N_k(\vec{r}, t)+\omega(N_k^{(0)}(\vec{r}, t)-N_k(\vec{r}, t)) \quad (1)$$

[1] Computer Science Department, University of Geneva, 1211 Geneva 4, Switzerland.
[2] To whom correspondence should be addressed; e-mail: Bastien.Chopard@cui.unige.ch

0022-4715/02/0400-0023/0 © 2002 Plenum Publishing Corporation

where τ is the time step of the simulation, ω the inverse of a relaxation time and $N_k^{(0)}$ the local equilibrium which is a function of the density $\rho = \sum_{i=0}^{z} m_k N_k$ and the fluid velocity $\vec{u} = \frac{1}{\rho} \sum_{i=1}^{z} m_k N_k \vec{v}_k$. The quantities m_k are weights associated with the lattice directions. See refs. 1, 6, and 7 for more information.

A lattice Boltzmann fluid is thus a virtual fluid made of fictitious mesoscopic particles evolving in a discrete space-time universe. It is well known that Eq. (1) produces the same behavior as that predicted by the Navier–Stokes equations.

In refs. 1, 8, and 9 we have investigated the possibility to use the LB framework to go beyond the fluid model and describe a virtual solid body. In our approach, a solid is made up of a collection of particles, locally connected through an elastic interaction, which can move (usually off-lattice) according to sensible physical laws, deform while keeping its integrity and possibly break if internal constraints become too large.

The purpose of this paper is to immerse such a solid object in a lattice Boltzmann fluid and study the properties of such a system. The interest is to obtain a fully mesoscopic model for a fluid-solid system, in which both the solid and the fluid are treated on the same footing and all interactions take place locally, at the level of the particles making up the solid or the fluid. Thus, our approach differs from that of Ladd, Behrend or Aidun[10–12] in which the solid suspended in the fluid is rigid and its motion is computed at a higher level of abstraction by aggregating the effect of the fluid around its surface.

The applications we might consider within this framework are fluid flows within flexible walls (e.g., blood flow in arteries), the effect of wind on solid structures (buildings), and a way to introduce non-Newtonian behavior in a flow.

The paper is organized as follows. In Section 2 the solid model and its basic properties are recalled. The interaction fluid-solid is described in Section 3 and some validation of the model are proposed in Section 4.

2. A LATTICE BOLTZMANN MODEL FOR A SOLID BODY

A simple, two-dimensional solid model can be defined as an array of particles connected according to a square topology. Each particle (i, j) is characterized by its spatial location $\vec{r}_{ij}(t) \in \mathbf{R}^2$ at the discrete time t and the list of neighbors it is connected to. A bulk particle is typically connected to four other particles (at North, West, South and East) but the shape of the solid boundary can be arbitrary and border particles may have three, two or even one neighbor.

An intuitive explanation of the rule describing the motion of the particle making up such a solid can be found in refs. 13, 1, 8, and 9. Here we explain the model in a more abstract way and give some of its important properties. It turns out that the dynamics of our solid is described by an LB equation having a similar structure as to (1). We refer the reader to a forthcoming paper for a complete account of the model[14] and the proofs of its properties.

Figure 1 gives an example of the type of solid body our model can deal with. A square sheet of particles with a given initial velocity keep bouncing over surrounding rigid walls. When a particle at the boundary of the solid reaches a wall, it is stopped and the solid starts deforming until the entire object has bounced back. When the solid and the wall do not interact, the center of mass of the solid follows a straight line, as it should for a body whose momentum is conserved.

2.1. Definition of the Model

To describe an object such as that of Fig. 1, we first label each particle with an index $\vec{\ell} = (i, j)$ and introduce vectors $\vec{c}_k$ (typically $\vec{c}_1 = (1, 0)$, $\vec{c}_2 = (0, 1)$, $\vec{c}_3 = (-1, 0)$, $c_4(0, -1)$) so that the neighbor of particle $\vec{\ell}$ in direction k is labeled $\vec{\ell} + \vec{c}_k$. The index k runs over all the links that connect a particle to its neighbors. For bulk particles in 2D, k runs from 1 to 4, but at the boundary several links may be missing.

The internal dynamics of our virtual solid is due to the forces $\vec{f}_k(\vec{\ell})$ acting on each particle $\vec{\ell} = (i, j)$ and caused by some idealized springs of rest length Δ_k connecting particles $\vec{\ell}$ and $\vec{\ell} + \vec{c}_k$. Figure 2 illustrates the situation

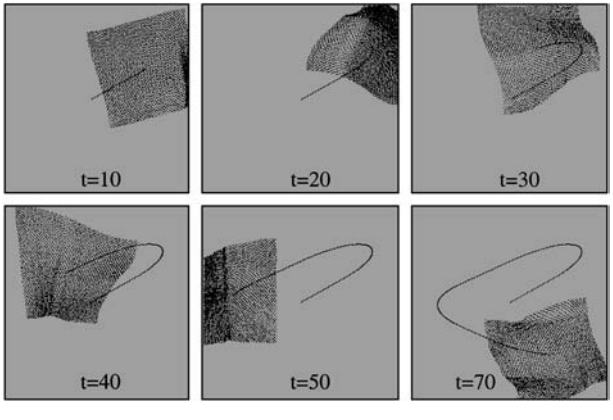

Fig. 1. Simulation of a 2D LB solid object with an initial momentum and moving in a container with rigid walls.

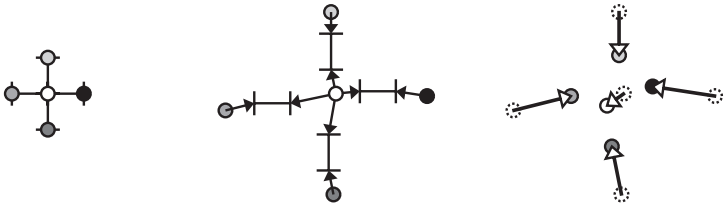

Fig. 2. The internal dynamics of a LB solid. The $\vec{f}_k$'s are interpreted as the forces acting on a particle due to the local deformation of the structure. These forces result in the motion of the particle which, in turn give rise to a redistribution of the forces to the nearest neighbors. On the left, a fragment of five particles in a rest configuration is shown; in the middle, the fragment is under strain; on the right, the particle displacement caused by the forces is displayed.

and Fig. 3 explain the symbols. Note that in this model, the springs have a fixed orientation.

Since elastic deformations in a solid propagate as a wave, we propose to describe the dynamics of the forces $\vec{f}_k$ using a LB formulation of a wave process. It can be shown[1, 15] that

$$\vec{f}_k(\vec{\ell}+\tau\vec{c}_k, t+\tau) = \vec{f}_k(\vec{\ell}, t)+\omega(\vec{f}_k^{(0)}(\vec{\ell}, t)-\vec{f}_k(\vec{\ell}, t)) \tag{2}$$

causes the quantities $\vec{f}_k$ to propagate as a wave provided that $\omega = 2$ and

$$\vec{f}_k^{(0)} = \frac{1}{2M}\vec{\Psi}+\frac{1}{2}\vec{c}_k J$$

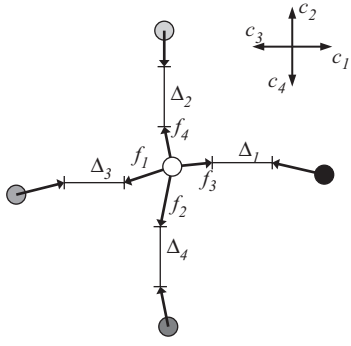

Fig. 3. Labeling of the forces and directions. By definition, the forces are labeled according to the direction through which the interaction has propagated. For instance, $\vec{f}_3(\vec{\ell})$ comes from particle $\vec{\ell}+\vec{c}_1$ through link $\vec{c}_3$. Finally, the quantities $\vec{\Delta}_k$ designate the spring at rest connecting particle $\vec{\ell}$ to $\vec{\ell}+\vec{c}_k$.

where the quantity $\vec{\Psi}_{\vec{\ell}}$ is

$$\vec{\Psi}_{\vec{\ell}}(t) = \sum_k \vec{f}_k(\vec{\ell}, t) \tag{3}$$

and the tensor J reads

$$J_{\alpha\beta} = \sum_k c_{k\alpha} f_{k\beta} \tag{4}$$

The quantity M is dependent of the particle and the number of neighbors it is connected to. The appropriate choice to satisfy the conservation laws[13, 14] is to consider a contribution of $1/2$ per link. Thus, if particle $\vec{\ell}$ has K neighbors, we define

$$M_{\vec{\ell}} = \frac{K}{2} \tag{5}$$

For the present 2D case, the number of links is smaller than or equal to 4, but this model extends easily to 3D. Also, note that a rest field $\vec{f}_0$ could also be introduced in the dynamics to tune the speed of sound.[1, 6] This possibility will not be discussed here.

Equation (2) is similar to Eq. (1) except that the fields $\vec{f}_k$ are vectors and do not need to be positively defined. In addition, the local equilibrium distribution is different of that of hydrodynamics in order to obtain a wave propagation. In particular, Eq. (2) is linear. Finally the condition $\omega = 2$ is necessary to ensure time reversal invariance and does not cause any numerical stability problems as long as one considers lattice topologies with links all of the same length, such as D2Q5, D2Q7, or D3Q7.

Assuming that an external force $\vec{F}_{\vec{\ell}}$ may be acting on each particle $\vec{\ell}$, Eq. (2) together with (3) and (4) can be cast in a more compact form

$$\vec{f}_i(\vec{\ell} + \vec{c}_i, t + \tau) = M_{\vec{\ell}}^{-1} \vec{\Psi}_{\vec{\ell}}(t) - \vec{f}_{i+2}(\vec{\ell}, t) + \frac{\vec{F}_{\vec{\ell}}(t)}{2M_{\vec{\ell}}} \tag{6}$$

The above equations describe how the internal forces evolve in the system. They also cause the particles to move. Whereas the force fields are attached to a fixed lattice topology, the particles may well move off-lattice. The rule of motion we propose for the particles is

$$\vec{r}_{\vec{\ell}}(t + \tau) = \vec{r}_{\vec{\ell}}(t) + \frac{\vec{\Psi}_{\vec{\ell}}(t)}{M_{\vec{\ell}}} + \frac{\vec{F}_{\vec{\ell}}(t)}{2M_{\vec{\ell}}} \tag{7}$$

where $\vec{r}_{\vec{\ell}}(t)$ denotes the location of particle $\vec{\ell}$.

A geometrical interpretation of this relation is given in ref. 1 for a particular case. A more formal proof is given by the fact that $\vec{\Psi}$ is a locally conserved quantity (see below) which can judiciously used to represent the momentum of each particle.

It is important to note that the above model is not invariant under rotation, due to the fixed orientation of the rest springs Δ_k and, for this reason, the present solid cannot freely rotate. This problem is related to the fact there is no simple theory of rotation for a non-rigid body. This problem is important for situations not entirely consisting of a translational motion and we shall return to it later in the text.

2.2. Properties

There are three important properties which follow from the equation of motion (6) and (7). They are related to momentum and energy conservation, and with a law relating the local deformation and the forces.

2.2.1. Momentum Conservation

If we consider a given site $\vec{\ell}$ at time t, the local forces $\vec{f}_i(\vec{\ell}, t)$ define the quantity $\vec{\Psi}$, as given by Eq. (3). After the interaction take place, there is a new distribution of forces leaving site $\vec{\ell}$. If we sum all these field emanating from the interaction at site $\vec{\ell}$, we obtain a quantity $\vec{\Psi}^{\text{out}} \equiv \sum_i \vec{f}_i(\vec{\ell}+\vec{c}_i, t+\tau)$ which can be computed easily. Simple algebra gives

$$\vec{\Psi}^{\text{out}} = \vec{\Psi} + \vec{F} \tag{8}$$

In other words, the variation of the quantity $\vec{\Psi}$ during one step is equal to the external force. Thus, in absence of force $\vec{F}$, the sum of $\vec{\Psi}$ over all particle is exactly conserved.

Due to property (8), it make sense to interpret $\vec{\Psi}$ as the momentum and to relate the displacement of the particle to $\vec{\Psi}$ as done in Eq. (7).

2.2.2. Energy Conservation

A second conserved quantity that can be defined in this model is

$$E_{\vec{\ell}}(t) = \sum_{i \geqslant 0} \vec{f}_i^{\,2}(\vec{\ell}, t) \tag{9}$$

that we shall interpret as the energy of node $\vec{\ell}$. We can easily compute how this quantity changes after one iteration. Following the same procedure as for the momentum (i.e., summing the contributions that flow to the neighbors), we obtain

$$E^{\text{out}} = E + (\vec{r}_{\vec{\ell}}(t+\tau) - \vec{r}_{\vec{\ell}}) \cdot \vec{F} \tag{10}$$

Thus, the variation of energy is equal to the work done by the external force. This justifies the terminology of energy.

2.2.3. Deformation

Finally, the dynamics of the model also implies that the following quantity

$$\vec{r}_{\vec{\ell}+\vec{c}_i}(t)-\vec{r}_{\vec{\ell}}(t)+\vec{f}_i(\vec{\ell}+\vec{c}_i,\,t)-\vec{f}_{i+2}(\vec{\ell},\,t)=\vec{\Delta}_i^0(\vec{\ell}) \tag{11}$$

is a constant of the motion. We interpret this quantity $\vec{\Delta}_i^0(\vec{\ell})$ as the equilibrium separation between particles $\vec{\ell}$ and $\vec{\ell}+\vec{c}_i$ because that is what it should be when the $\vec{f}$'s are zero. Note that Eq. (11) should be used to specify correctly the relation between the initial position of the particles and the f's at time $t=0$.

2.3. Units

The equations in the last section have been given without units. Any physical quantity $\tilde{q}$ has a dimensionless counterpart q obtained as $q\equiv\frac{\tilde{q}}{\chi}$, where χ is a factor containing the units of $\tilde{q}$.

In our problem, we have three fundamental scales that are λ for [meters], κ for [kilograms] and τ for [seconds].

The correspondence between the dimensionless quantities we have used so far and the physical ones is given in Table I where each variable is given with the units it bears. It is therefore possible by simple substitution to retrieve units in all of the above equations.

3. SOLID–FLUID INTERACTION

In this section we define the interaction between the particles making up the solid body and the surrounding fluid. We assume that the fluid is

Table I. Units of the Variables Used in the Model

variable	symbol	unit
neighbors	K	—
local force fields	$\vec{f}_i$	$\kappa\lambda\tau^{-2}$
mass	M	κ
force	$\vec{F}$	$\kappa\lambda\tau^{-2}$
momentum	$\vec{\Psi}$	$\kappa\lambda\tau^{-1}$
energy	E	$\kappa\lambda^2\tau^{-2}$
position	$\vec{r}$	λ
equilibrium separation	$\vec{\Delta}_i^0$	λ

described by a LB model, as presented in Section 1. The interaction we consider is based on a local exchange of momentum between solid and fluid particles.

The fluid particles live on a regular lattice (e.g., D2Q9[16]) but the solid particles are typically off lattice. Therefore each solid particle exchange its momentum with the fluid element located on the nearest lattice point.

Let t_+ denote the post-collision time, i.e., the time just before the fluid fields N_k and solid forces $\vec{f}_k$ are streamed to the corresponding neighbors. Let $\Delta\vec{P}$ represent the amount of momentum exchanged between a pair of solid–fluid particles. This quantity, computed with the pre-collision fields, can be introduced in the dynamical equations (1) and (6) in the following way

$$N_i(\vec{r}+\tau\vec{v}_i, t+\tau) = N_i(\vec{r}, t_+) + \frac{1}{C_2}\vec{v}_i \cdot \Delta\vec{P} \tag{12}$$

and

$$\vec{f}_i(\vec{r}+\vec{c}_i, t+\tau) = \vec{f}_i(\vec{r}, t_+) - \tfrac{1}{4}\Delta\vec{P} \tag{13}$$

where C_2 is the lattice coefficient defined as $\sum_k m_k v_{k\alpha} v_{k\beta} = C_2\delta_{\alpha\beta}$. It is easy to check that, with these relations, the fluid momentum $\rho\vec{u} = \sum_k m_k \vec{v}_k N_k$ increases by an amount $\Delta\vec{P}$ while the solid momentum $\vec{\Psi} = \sum_k \vec{f}_k$ decreases by the same quantity.

The last question is to determine the value $\Delta\vec{P}$. We choose to compute this value so that, after collision between a solid particle and a fluid element, both have the same velocity. In other words, we impose a no-slip condition at the fluid-solid interface. The solution is

$$\Delta\vec{P} = Z(\vec{u}_s - \vec{u}_f) \tag{14}$$

where $1/Z = (1/\rho + 1/M)$ and $\vec{u}_s$ and $\vec{u}_f$ are respectively the speeds of the solid and fluid particles before interaction. The quantities ρ and M denote the fluid density and the mass of the solid particle. The mass M has already been defined above and the fluid density is given by its standard expression $\rho = \sum_i N_i(\vec{r}, t)$.

The justification of Eq. (14) can be checked as follows: the fluid momentum after interaction is $\rho\vec{u}_f + Z(\vec{u}_s - \vec{u}_f)$ and, thus its velocity is

$$\vec{u}'_f = \vec{u}_f + \frac{M}{M+\rho}(\vec{u}_s - \vec{u}_f)$$

Similarly, the momentum of the corresponding solid particle is, after interaction, $M\vec{u}_s - Z(\vec{u}_s - \vec{u}_f)$. Therefore, its speed is

$$\vec{u}'_s = \vec{u}_s - \frac{\rho}{M+\rho}(\vec{u}_s - \vec{u}_f)$$

and, thus, $\vec{u}'_s - \vec{u}'_f = 0$.

Note that the solid objects we have defined here are permeable in the sense that fluid particles can penetrate between the solid particles, which is also the case for Ladd and Behrend's models.[10, 11] Figure 4 shows that the fluid which penetrate inside a plate moving in a fluid rapidly take the same speed as the solid. Therefore the porosity of our solid has no important effect.

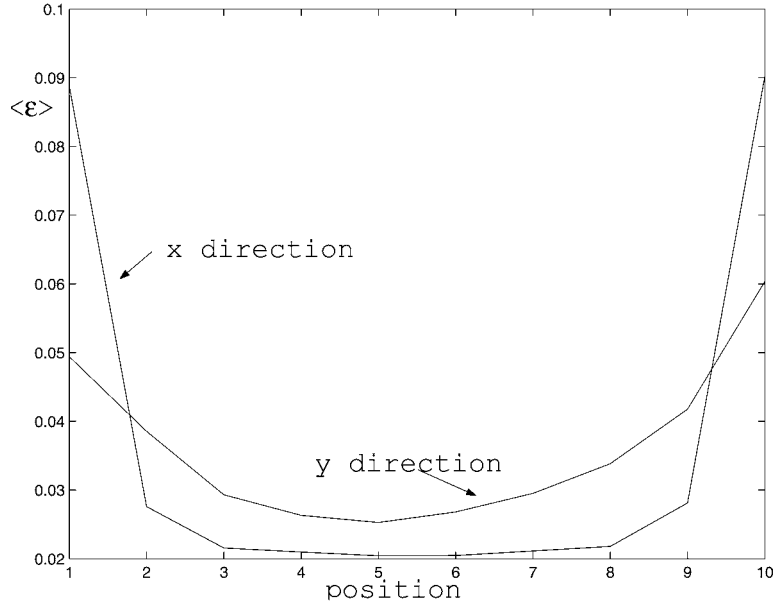

Fig. 4. The amount of fluid inside a solid. For a 10×10 square solid under traction in the x direction, we measure the normalized difference $\epsilon_{x,y} = |\frac{u_s - u_f}{u_s}|_{x,y}$ of velocity between a solid and a fluid site. The plot is that of the mean difference $\langle \epsilon \rangle$ in both directions. We observe that apart for a thin layer on the boundaries facing the flow, the fluid inside a moving solid has the same velocity.

4. SOME NUMERICAL EXPERIMENTS

The goal of this section is to validate the solid–fluid interaction described in Section 2 through a drag experiment and then study a "polymerized" fluid. In all cases, a D2Q7 lattice with $\omega = 1.0$ is used to model the fluid.

4.1. Drag Coefficient

The situation we consider is a drag experiment with a disk whose internal particles are subject to an external force $\vec{F}$ introduced as shown in (6). This force accelerates the object in a 2D channel filled with a LB fluid whose viscosity is known to be[1, 16] $\nu \propto (1/\omega - 1/2)$. As the solid moves, each of its particle exchange momentum with the surrounding fluid, as explained in Section 3. The channel is periodic along the horizontal direction and has a no-slip boundary conditions at the upper and lower walls obtained with a bounce-back scheme.

It is common to consider the so-called drag coefficient[17, 18]

$$c_d = \frac{F}{\rho u_\infty^2 D}$$

where D is the disk diameter. It is well known from Stokes law[17, 18] that for a cylinder

$$\text{if} \quad \text{Re} \ll 10^2 \qquad \text{then} \quad c_d \propto \frac{1}{\text{Re}} \tag{15}$$

where Re is the Reynolds number.

In our simulations, we compute the cylinder's velocity u_∞ by considering that at small velocities the velocity of the cylinder obeys

$$\frac{du}{dt} = -au(t) + F$$

in agreement with (15) and whose solution is

$$u(t) = \frac{F}{a}(1 - e^{-at})$$

Figure 5 (left) shows a fit to such a behavior for the velocity of the cylinder.

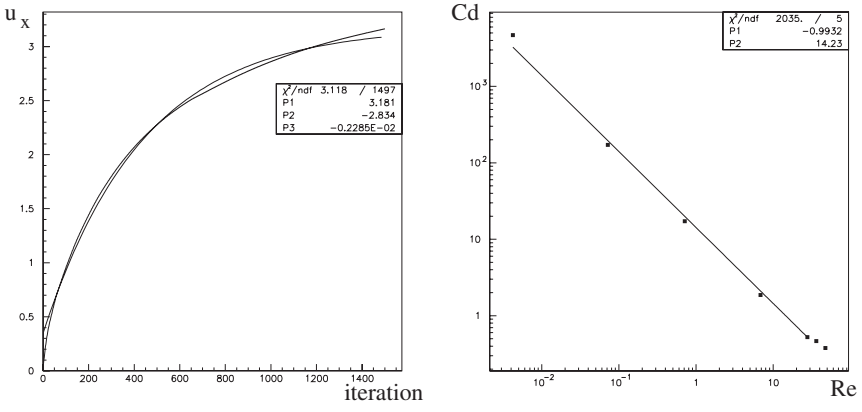

Fig. 5. Drag simulation: (right) the evolution of the velocity of the cylinder follows $u(t) = \frac{F}{a}(1 - e^{-at})$. (left) Stokes law for a cylinder; up to Reynolds number of a 10^2 $\mathrm{Cd} \propto \mathrm{Re}^{-1}$, units are arbitrary.

The drag force F is the only parameter we choose to adjust the value of our Reynolds number. Figure 5 (right) shows the results of our drag experiments. The correct relation between the drag coefficient and the Reynolds number as expected by Stokes law is observed and corresponds to experimental results reported in textbook.[17] As the Reynolds number approaches the value of 10^2 where Stokes law is in fact no longer valid, a small deviation can effectively be seen. Note that in this experiment, no important deformation of the solid has been observed while in motion in the fluid.

4.2. A Polymerized Fluid

The experiment we perform consists in placing a set of one-dimensional solids (i.e., chains of particles, or pseudo-polymer) in a shear flow $\vec{u} = (u_x(y), 0)$ with $\partial_y u_x(y) \neq 0$. We consider the following three situations: first the chains are perpendicular to the flow and extend over several fluid layers; second, the chains are parallel to the flow; finally a mixed system of parallel and perpendicular polymer is investigated. In all cases, we study the properties of the mean velocity profile of the fluid along the channel which for a Newtonian fluid under shear stress follows

$$\tau_{xy} \sim \nu \frac{\partial u_x}{\partial y}$$

where τ_{xy} is the shear strees imposed on the fluid.

In the perpendicular case, see Fig. 6 (left), the velocity profile appears to be flat compared to the free case. The profile is in fact still that of a

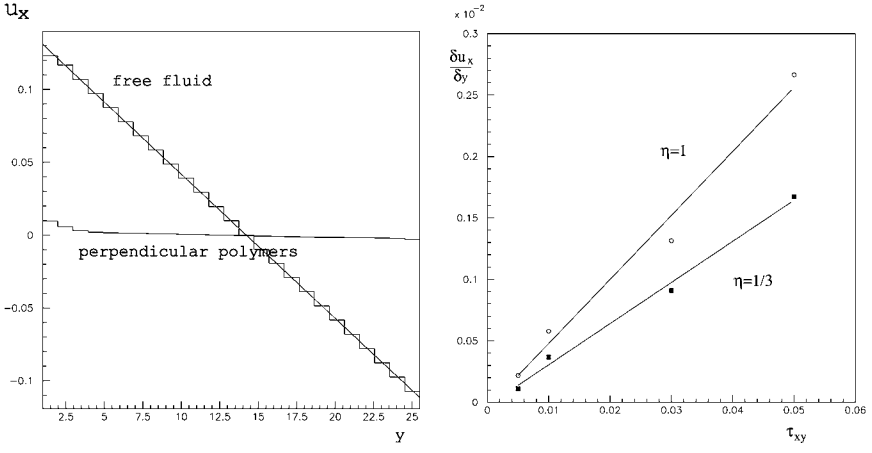

Fig. 6. (left) Velocity profiles for a fluid free of polymers and a fluid with 2000 polymers perpendicular to the flow. The flat profiles is in fact still a linear shear flow profile. The gradient differs of two orders of magnitude: the free case exhibits a slope of 0.01 while for the perpendicular case it is worth 0.00022 leading to a apparent viscosity 45 times higher. (right) The dependency of the gradient of u_x as a function of shear stress. The relation is linear, however the linearity constant depends on the ratio η between parallel and perpendicular polymers. The two plots are for a total of 2000 polymers and $\eta = 1$ and $\eta = 1/3$.

Newtonian shear flow but with a proportionality constant nearly two orders of magnitude lower. The apparent viscosity of the fluid is therefore strongly increased by the presence of perpendicular polymers. This can be understood from the fact that the perpendicular chains couple layers of fluids with different velocities and tend to force them to have the same speed.

In the parallel case, we start with a fluid at rest and a given density of parallel polymers also at rest. We observe that the stationary velocity gradient is identical to the case of the free fluid. This is expected since the polymers are now aligned with the fluid layers and do not prevent a gradient to set up.

However, the time it takes for the fluid to relax to this stationary velocity profile is dependent of the parallel polymer concentration. To measure the characteristic relaxation time, we simply fit the velocity profile with a first order polynomial and look at the evolution of the chi-square χ_2 coefficient during time. The time evolution of this coefficient can be fitted with an exponential whose time constant $1/\gamma$ is shown in Fig. 7, for various values of the number of polymers in the system. Therefore, the presence of parallel chains of particles slows down the response of the fluid to an external stress.

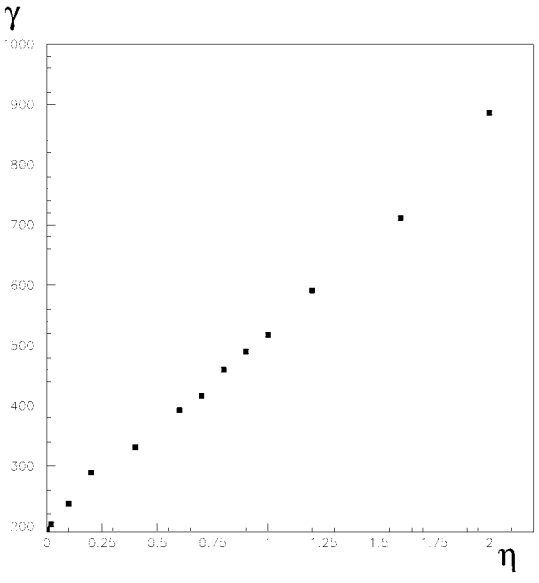

Fig. 7. The characteristic relaxation time to the linear shear profile as a function of polymer concentration η. The plot shows the time constant γ. The value of η means the number of solid particle per fluid cell.

Finally, we study a mixed system of parallel and perpendicular polymers. Given a constant number of polymers, we look at the influence of the shear stress on the velocity profile for two different ratios of parallel and perpendicular polymer densities. As expected from the purely perpendicular case, the velocity profile is several order of magnitude lower than the free case. However, it does depend linearly with the shear stress as expected from a Newtonian fluid, Fig. 6 (right). The proportionality constant, i.e., the viscosity, however depends on the ratio of parallel and perpendicular chains. Therefore, by introducing a mechanism enabling a rotation of the polymers, which is not yet the case in this model, we expect to be able to model a non Newtonian behavior for the fluid. Of importance will be the characterisic time for the response of the polymers to a local velocity gradient and the time for the rotation in order to adjust the viscoelastic properties.

It is important to remember that an important issue of this model is to keep all components at the same level of description. At this point, introducing rotations, i.e., angular momentum, in the LB model of the solid has not yet been possible and may not be for theoretical reasons. We might therefore consider the possibility to put an ad hoc mechanism, similar to that used by Ladd,[10] in which the total torque is considered to produce a global rotation of the object.

5. CONCLUSIONS

We have introduced a mesoscopic model for solid bodies whose internal "atoms" move according to a LB dynamics. Mass, momentum and energy can be defined for such an object and these quantities behave as expected for a real solid. However, no conserved angular momentum can be introduced in the current version of the model.

The complete description of this LB solid will be given elsewhere[14] and the application of the model to fracture phenomena is given in ref. 9. The main goal of the present paper is to investigate the behavior of such solid object in suspension in a LB fluid. The results is that both large scale solid suspensions of arbitrary shapes and the fluid are described at the same mesoscopic level. Thus interaction between fluid elements and solid particles are naturally implemented through a momentum exchange. The amount of momentum exchanged is chosen so as to ensure a no-slip condition at the solid–fluid interface. As a validation, we have numerically studied a LB solid dragged by an external force in a LB fluid. The properties are in agreement with the expected behavior.

Finally we have shown that introducing a population of "polymers," i.e., 1d chains of our LB solid, in a shear flow can modify the velocity profile. The resulting fluid is still Newtonian, however the proportionality constant between stress and velocity gradient depends on the ratio of polymers with parallel and perpendicular orientation to the flow. By introducing a mechanism allowing for the rotation of the polymers in an extension of this model, we expect to observe a non Newtonian behavior of the fluid.

Among the possible applications of the model we plan to develop, we can mention the problem of a fluid flow contained in flexible wall such as blood flow in artery (provided one prevents the fluid to penetrate the solid), or applications to study the deformation of flexible objects in a flow (e.g., behavior of seaweeds in water current, or the impact of wind on construction).

REFERENCES

1. B. Chopard and M. Droz, *Cellular Automata Modeling of Physical Systems* (Cambridge University Press, 1998).
2. S. Chen and G. D. Doolen, Boltzmann methods for fluid flows, *Annu. Rev. Fluid Mech.* **30**:329 (1998).
3. Sauro Succi, *The Lattice Boltzmann Equation, For Fluid Dynamics and Beyond* (Oxford University Press, 2001).
4. B. Boghosian and collaborators, eds., *Proceedings of the 7th Conference on Discrete Simulation of Fluid Dynamics, Oxford, 1998*, Vol. 9, Int. J. Mod. Phys. C (1998).

5. Yu Chen *et al.*, eds., *The 9th International Conference on the Discrete Simulation of Fluid Dynamics, Tokyo, 1999*, Vol. 129, Computer Physics Communications (2000).
6. B. Chopard, P. Luthi, and A. Masselot, *Cellular Automata and Lattice Boltzmann Techniques: An Approach to Model and Simulate Complex Systems* (1998), http://cui.unige.ch/~chopard/CA/Book/related.html
7. B. Chopard, A. Masselot, and A. Dupuis, A lattice gas model for erosion and particles transport in a fluid, in *Proceedings of the LGA'99 Conference, Tokyo*, Vol. 129, Yu Chen *et al.*, eds., Computer Physics Communications (2000), pp. 167–176.
8. B. Chopard and P. O. Luthi, Lattice Boltzmann computations and applications to physics, *Theoretical Computer Science* **217**:115–130 (1999).
9. B. Chopard and S. Marconi, A lattice Boltzmann wave model applied to fracture phenomena, in *14th Int. Symposium of Mathematical Theory of Network and Systems, MTNS 2000* (University of Perpigan, France, 2000), http://cui.unige.ch/~chopard/FTP/Fracture/
10. A. J. C. Ladd, Numerical simulation of particulate suspensions via a discretized Boltzmann equation, *J. Fluid Mech.* **271**:285, 310 (1994).
11. O. Behrend, Solid–fluid boundaries in particle suspension simulations via the lattice Boltzmann method, *Phys. Rev. E* **52**:1164–1175 (1995).
12. C. K. Aidun and Y. Lu, Lattice Boltzmann simulation of solid particles suspended in a fluid, *J. Statist. Phys.* **81**:49–59 (1995).
13. B. Chopard, A cellular automata model of large scale moving objects, *J. Phys. A* **23**:1671–1687 (1990).
14. S. Marconi and B. Chopard, A lattice Boltzmann model for the mechanics of a discrete solid body, in preparation.
15. B. Chopard, P. O. Luthi, and Jean-Frédéric Wagen, A lattice Boltzmann method for wave propagation in urban microcells, *IEE Proceedings—Microwaves, Antennas and Propagation* **144**:251–255 (1997).
16. Y. H. Qian, S. Succi, and S. A. Orszag, Recent advances in lattice Boltzmann computing, in *Annual Reviews of Computational Physics III*, D. Stauffer, ed. (World Scientific, 1996), pp. 195–242.
17. D. J. Tritton, *Physical Fluid Dynamics* (Clarendon Press, 1988).
18. Alexander J. Smits, *A Physical Introduction to Fluid Mechanics* (Wiley, 2000).